Effects of the BET-inhibitor, RVX-208 on the HDL lipidome and glucose metabolism in individuals with prediabetes: A randomized controlled trial

Andrew L. Siebel, Si Khiang Trinh, Melissa F. Formosa, Piyushkumar A. Mundra, Alaina K. Natoli, Medini Reddy-luthmoodoo, Anmar A. Khan, Andrew L. Carey, Gerrit van Hall, Claudio Cobelli, Chiara Dalla-Man, Jim D. Otvos, Kerry-Anne Rye, Jan Johansson, Allan Gordon, Norman C.W. Wong, Dmitri Sviridov, Philip Barter, Stephen J. Duffy, Peter J. Meikle, Bronwyn A. Kingwell

PII: S0026-0495(16)00056-1
DOI: doi: 10.1016/j.metabol.2016.03.002
Reference: YMETA 53392

To appear in: *Metabolism*

Received date: 22 October 2015
Accepted date: 3 March 2016

Please cite this article as: Siebel Andrew L., Trinh Si Khiang, Formosa Melissa F., Mundra Piyushkumar A., Natoli Alaina K., Reddy-luthmoodoo Medini, Khan Anmar A., Carey Andrew L., van Hall Gerrit, Cobelli Claudio, Dalla-Man Chiara, Otvos Jim D., Rye Kerry-Anne, Johansson Jan, Gordon Allan, Wong Norman C.W., Sviridov Dmitri, Barter Philip, Duffy Stephen J., Meikle Peter J., Kingwell Bronwyn A., Effects of the BET-inhibitor, RVX-208 on the HDL lipidome and glucose metabolism in individuals with prediabetes: A randomized controlled trial, *Metabolism* (2016), doi: 10.1016/j.metabol.2016.03.002

Effects of the BET-inhibitor, RVX-208 on the HDL lipidome and glucose metabolism in individuals with prediabetes: a randomized controlled trial

Andrew L. Siebel[1], Si Khiang Trinh[1], Melissa F. Formosa[1], Piyushkumar A. Mundra[1], Alaina K. Natoli[1], Medini Reddy-luthmoodoo[1], Kevin Huynh[1], Anmar A. Khan[1], Andrew L. Carey[1], Gerrit van Hall[3], Claudio Cobelli[4], Chiara Dalla-Man[4], Jim D. Otvos[5], Kerry-Anne Rye[6], Jan Johansson[7], Allan Gordon[7], Norman C.W. Wong[7], Dmitri Sviridov[1], Philip Barter[6], Stephen J. Duffy[2], Peter J. Meikle[1], Bronwyn A. Kingwell*[1]

[1]Baker IDI Heart and Diabetes Institute, Melbourne, Australia;
[2]Heart Centre, The Alfred Hospital, Melbourne, Australia;
[3]Department of Biomedical Sciences, University of Copenhagen, Copenhagen, Denmark;
[4]Department of Information Engineering, University of Padova, Padova, Italy;
[5]LabCorp, Raleigh, USA;
[6]School of Medical Sciences, Faculty of Medicine, University of New South Wales, Sydney, Australia;
[7]ResVerlogix Corp., San Francisco, USA.

Abbreviated title: RVX-208, the HDL lipidome and glucose metabolism

Word count: 4,238

Number of figures and tables: 7

Corresponding author:
Professor Bronwyn A. Kingwell, PhD
Metabolic & Vascular Physiology
Baker IDI Heart & Diabetes Institute
P.O. Box 6492, St Kilda Road Central
Melbourne, Victoria, 8008
AUSTRALIA
Phone: +61 3 8532 1518, Fax: + 61 3 8532 1160
Email: bronwyn.kingwell@bakeridi.edu.au

Conflict-of-interest/financial disclosure statement

JJ & NCWW are employees, share- and option holders of Resverlogix Corporation. JDO is employed by LabCorp. BAK received a research grant and travel support from Resverlogix Corporation. This study was supported by Resverlogix Corp., the National Health & Medical Research Council (NHMRC) of Australia (APP1065462) to BAK, SJD and ALS, and in part by the Victorian Government's Operational Infrastructure Support (OIS) Program. BAK, DS and PJM are all supported by NHMRC Research Fellowships.

Abstract

Aims

High-density lipoprotein (HDL) and apolipoprotein A-I (apoA-I) can modulate glucose metabolism through multiple mechanisms. This study determined the effects of a novel bromodomain and extra-terminal (BET) inhibitor (RVX-208) and putative apoA-I inducer on lipid species contained within HDL (HDL lipidome) and glucose metabolism.

Materials and methods

Twenty unmedicated males with prediabetes received 100mg b.i.d RVX-208 and placebo for 29-33 days separated by a wash-out period in a randomized, cross-over design trial. Plasma HDL-cholesterol and apoA-I were assessed as well as lipoprotein particle size and distribution using NMR spectroscopy. An oral glucose tolerance test (OGTT) protocol with oral and infused stable isotope tracers was employed to assess postprandial plasma glucose, indices of insulin secretion and insulin sensitivity, glucose kinetics and lipolysis. Whole plasma and HDL lipid profiles were measured using mass spectrometry.

Results

RVX-208 treatment for 4 weeks increased 6 sphingolipid and 4 phospholipid classes in the HDL lipidome ($p \leq 0.05$ versus placebo), but did not change conventional clinical lipid measures. The concentration of medium-sized HDL particles increased by 11% (P=0.01) and small-sized HDL particles decreased by 10% (P=0.04) after RVX-208 treatment. In response to a glucose load, after RVX-208 treatment, plasma glucose peaked at a similar level to placebo, but 30 minutes later with a more sustained elevation (treatment effect, P=0.003). There was a reduction and delay in total (P=0.001) and oral (P=0.003) glucose rates of appearance in plasma and suppression of endogenous glucose production (P=0.014) after RVX-208 treatment. The rate of glucose disappearance was also lower following RVX-208 (P=0.016), with no effect on glucose oxidation or total glucose disposal.

Conclusions

RVX-208 increased 10 lipid classes in the plasma HDL fraction, without altering the concentrations of either apoA-I or HDL-cholesterol (HDL-C). RVX-208 delayed and reduced oral glucose absorption and endogenous glucose production, with plasma glucose maintained via reduced peripheral glucose disposal. If sustained, these effects may protect against the development of type 2 diabetes.

ClinicalTrials.gov identifier: NCT01728467

Keywords: Clinical trial; Glucose metabolism; Glycemic control; Type 2 diabetes; High-density lipoprotein; Prediabetes

Abbreviations

ALT – Alanine aminotransferase

AMPK – AMP-activated protein kinase

ApoA-I – Apolipoprotein A-I

ApoA-II – Apolipoprotein A-II

AST – Aspartate aminotransferase

BET – Bromodomain and extra-terminal

BH – Benjamini-Hochberg

BMI – Body mass index

CE – Cholesteryl ester

Cer – Ceramide

CETP – Cholesteryl ester transfer protein

COH – Free cholesterol

DG – Diacylglycerol

DHC – Dihexosylceramide

dhCer – Dihydroceramide

DI – Disposition index

eGFR – Estimated glomerular filtration rate

FBE – Full blood examination

GGT – Gamma-glutamyl transpeptidase

GIP – Gastric inhibitory polypeptide

GLP-1 – Glucagon-like peptide 1

GM3 – GM3 ganglioside

HbA_{1c} – Glycated hemoglobin

HDL – High-density lipoprotein

HDL-C – HDL-cholesterol

hsCRP – High-sensitivity C-reactive protein

IDL – Intermediate-density lipoprotein

LCAT – Lecithin-cholesterol acyltransferase

LC-ESI-MS/MS – Liquid chromatography, electrospray ionisation tandem mass spectrometry

LDL – Low-density lipoprotein

LDL-C – LDL-cholesterol

LFT – Liver function test

LPC – Lysophosphatidylcholine

LPC(O) – Lysoalkylphosphatidylcholine

LPE – Lysophosphatidylethanolamine

LPI – Lysophosphatidylinositol

MCH – Mean corpuscular hemoglobin

MCHC – Mean corpuscular hemoglobin concentration

MCV – Mean corpuscle volume

MHC – Monohexosylceramide

NMR – Nuclear magnetic resonance

OGTT – Oral glucose tolerance test

PC – Phosphatidylcholine

PC(O) – Alkylphosphatidylcholine

PC(P) – Alkenylphosphatidylcholine

PE – Phosphatidylethanolamine

PE(O) – Alkylphosphatidylethanolamine

PE(P) – Alkenylphosphatidylethanolamine

PG – Phosphatidylglycerol

PI – Phosphatidylinositol

PS – Phosphatidylserine

R_a – Rate of appearance

R_d – Rate of disappearance

RDW – Red cell distribution width

rHDL – Reconstituted HDL

S1P – Sphingosine-1-phosphate

S_I – Insulin sensitivity index

SM – Sphingomyelin

T2DM – Type 2 diabetes mellitus

TG – Triglycerides/triacylglycerides

THC – Trihexosylceramide

U&E – Urea and electrolytes

VLDL – Very low-density lipoprotein

1. Introduction

HDL and its major apolipoprotein, apoA-I can directly modulate glucose metabolism through multiple mechanisms [1-3]. In the clinical setting, acute HDL elevation via short-term reconstituted HDL (rHDL) infusion [1] and chronically raising HDL via a cholesteryl ester transfer protein (CETP) inhibitor [3] reduce blood glucose in individuals with type 2 diabetes mellitus (T2DM). This is underpinned by at least two known mechanisms, namely increased insulin secretion [1, 4, 5] and enhanced skeletal muscle glucose uptake via an AMP-activated protein kinase (AMPK)-mediated mechanism [1]. HDL may also act via a third mechanism to increase insulin sensitivity via lipid removal and anti-inflammatory actions in metabolic tissues [6]. These newly described roles of HDL relating to glucose metabolism [2] suggest therapies that target HDL and/or apoA-I may have relevance in the management of T2DM.

The focus of HDL therapies has evolved in the light of recent data showing that HDL particle number, composition and function relate more closely to cardiovascular outcome than standard clinical measures of HDL-C content [7-9]. As a result, compounds targeting apoA-I are of particular interest due to their potential to increase HDL particle number and favourably alter the lipid composition and function of existing particles [8, 10]. RVX-208 is an orally active small molecule which induces apoA-I through selective inhibition of BET proteins [11-13]. In African green monkeys, 60mg/kg RVX-208 increased plasma apoA-I and HDL-C by 53% and 97% respectively after 28 days treatment [11]. In a follow-up phase I clinical trial in healthy volunteers RVX-208 (1 – 20 mg/kg/day) treatment for 7 days induced a 10% increase in plasma apoA-I and an 11% increase in the cholesterol efflux capacity of post-treatment plasma. To minimize potential liver transaminase elevations in humans, lower doses (100 – 150 mg b.i.d) of RVX-208 inducing more modest elevations in plasma apoA-I levels (3 – 6%) and HDL-C (6 – 8%) over a 12 week period have been investigated, with no

evidence of hepatotoxicity [14]. Beyond the effects of RVX-208 on clinical lipid parameters, modification of the relative quantity of the hundreds of lipid species within HDL is one possible mechanism mediating the functional properties of HDL.

The objectives of the current study were to determine the effects of RVX-208 on the HDL lipidome and postprandial glucose metabolism in individuals with prediabetes following a glucose load. Effects on glucose kinetics, insulin secretion and whole-body insulin sensitivity were determined during a modified frequently sampled oral glucose tolerance test (OGTT) [15], incorporating stable isotope tracers.

2. Material and methods

2.1 Patient population and screening

Twenty males aged 38 – 69 years with prediabetes based on WHO criteria (fasting blood glucose 6.1 – 6.9mmol/L and/or 2h blood glucose 7.8 – 11.0mmol/L after a 75g oral glucose load), body mass index (BMI) of 25 – 40 kg/m^2 and HDL-C levels ≤ 1.4mmol/L were enrolled. Smoking, previous history of major illness and any prescription or over-the-counter medications were all exclusion criteria (See Supplemental Figure 1 for CONSORT diagram). Patient characteristics and demographics are presented in Table 1. The study was approved by the Alfred Hospital Ethics Committee, performed in accordance with the Declaration of Helsinki (2008) and written informed consent was obtained from all participants.

For all visits, volunteers were required to attend The Alfred Hospital in the morning, following an overnight fast as well as having abstained from alcohol and caffeine for 24 hours. At visit 1 (screening) general health was checked by the study doctor and height, weight, waist and hip circumference and family T2DM history were recorded together with general lifestyle habits (e.g. exercise, smoking, alcohol). A 12-lead electrocardiogram was also performed. Circulating triglycerides (TG), total cholesterol, HDL-C and low-density lipoprotein-cholesterol (LDL-C) concentrations, liver function (LFT), kidney function/urea and electrolytes (U&E) and full blood examination (FBE) were all assessed to ensure that each individual met inclusion criteria. Volunteers then underwent a standard 2h oral OGTT.

2.2 Study design

This was a randomized, double-blind, placebo-controlled, cross-over study, where the Clinical Trials Pharmacy at The Alfred Hospital (Melbourne, Australia) was responsible for the dispensing of study drug to each participant at visit 2 and visit 5 in accordance with the

randomization list provided by the Sponsor. A simplified overview of the study design is presented in Figure 1. Participants received 100mg b.i.d (twice daily) RVX-208 and placebo each for 29 – 33 days separated by a wash-out period of 21 – 35 days in a randomized, cross-over design. Baseline fasting blood samples were taken prior to each intervention at visit 2 and visit 5 (pre-treatment) for plasma and lipidomic analyses. The fasting measures were repeated at visit 4 and visit 7 (post-treatment). At visit 3 and visit 6, a frequently sampled OGTT was performed after both the RVX-208 and placebo interventions. On these days, body weight was measured before catheters were inserted into antecubital veins of both arms for administration of stable isotope tracers and blood sampling. Fasting blood glucose was measured (T = -120 min) on an automated blood glucose analyzer (Radiometer, Copenhagen, Denmark). The left arm catheter was used to administer a constant infusion of [6,6-$^{2}H_{2}$]D-glucose, while the right arm catheter was used for blood sampling. Tracers were purchased from Cambridge Isotope Laboratories (Cambridge, MA), tested for sterility and pyrogenicity and prepared under aseptic conditions.

2.3 Blood and plasma analyses

Serum triglycerides, total cholesterol, HDL-C and LDL-C were measured using enzymatic assays on the Abbott Archicentre ci16200 autoanalyzer. High-sensitivity C-reactive protein (hsCRP) was measured by immunoturbidimetric assay as previously described [16], fructosamine by a rate assay on the Beckman Coulter DXC800 analyzer and whole blood HbA_{1c} by boranate affinity HPLC on the Trinity Premier Hb9210 analyzer. LFT, U&E and FBE were assessed throughout the trial on fasting blood samples by the Alfred Pathology Service using standard clinical assay techniques using either the Abbott Archicentre ci16200 or Beckman Coulter DXH800 analyzer. C-peptide and insulin analyses were conducted using chemiluminescent microparticle immunoassays on the Abbott Archicentre ci16200 analyzer.

Plasma apoA-I and apoA-II concentrations were determined immunoturbidometrically using sheep anti-human apoA-I and apoA-II polyclonal antibodies on the Beckman Coulter AU480 analyzer [17]. Human ELISA kits were used to measure gastric inhibitory polypeptide (GIP; EZHGIP-54K, Millipore Australia, Kilsyth, VIC, Australia) and glucagon-like peptide 1 (GLP-1; EZGLP1T-36K, Millipore Australia) plasma concentrations as previously described [5].

2.4 HDL preparation for lipidomic analysis

Fasting blood from participants was collected into EDTA tubes and immediately centrifuged (1,500 x *g*, 10 min, 4°C), plasma removed and stored at -80°C. The HDL fraction was isolated from 1mL of plasma by density gradient ultracentrifugation (Beckman Coulter Optima MAX-TL ultracentrifuge) adapted from [18] and detailed in Supplemental Materials and Methods.

2.5 Lipidomic analysis by liquid chromatography–mass spectrometry analysis

Lipidomic analysis was performed on post-intervention (RVX-208 and placebo) HDL fractions using liquid chromatography, electrospray ionisation tandem mass spectrometry (LC-ESI-MS/MS) on an Agilent 1200 LC system coupled to an API 4000 QTRAP (Applied Biosystems) mass spectrometer. Conditions for LC-ESI-MS/MS and quantification details are in the Supplemental Materials and Methods. Results are expressed as nmol/mg apoA-I for the HDL fraction. Data for a total of 342 lipids from 24 classes and subclasses were obtained and analyzed. Three lipid species (dihydroceramide (dhCer) 20:0, PC(P-30:0) and DG 16:0 22:5) were excluded from the HDL fraction analysis, as they were not detectable in this fraction. Two participants were excluded from the HDL fraction analysis; one subject was excluded due to failed lipidomic analysis and another due to failed ELISA analysis of apoA-I.

2.6 Nuclear magnetic resonance spectroscopic lipoprotein analysis

Lipoprotein particle size profiles and nuclear magnetic resonance (NMR) spectra of pre- and post-treatment fasting plasma samples were acquired at 47°C on a 400-MHz clinical NMR analyzer and measured using the LipoProfile-3 algorithm at LabCorp (Raleigh, NC) [19]. Lipoprotein (very low-density lipoprotein (VLDL)/chylomicron, low-density lipoprotein (LDL), intermediate-density lipoprotein (IDL) and HDL particle subclasses and total triglyceride (TG) concentration were quantified as described in the Supplemental Materials and Methods.

2.7 Glucose kinetics and oxidation

On the days of the frequently sampled OGTT (visits 3 and 6; Figure 1), a 2h period was allowed for the [6,6-$^{2}H_2$]D-glucose to reach steady-state levels in the blood. A priming bolus of [^{13}C]sodium bicarbonate (1.5μmol/kg) was also given 10 min prior to participants ingesting a drink at T = 0 min containing 71g glucose and 4g of [U-^{13}C]D-glucose to trace the ingested glucose. Blood samples were collected 30 and 15 mins before the commencement of the OGTT and at T = 0 min to determine glucose kinetics in the basal state. Blood samples were then taken every 10 min for the first 30 min post-glucose ingestion and thereafter every 15 min for determination of plasma glucose and tracer enrichment as well as plasma insulin and serum C-peptide. Plasma glucose concentration and enrichment were measured using LC-MS/MS and a hexobenzoyl derivatisation method, as described previously [20, 21]. Glucose kinetics were calculated using a non-steady state single-pool model as described previously [22]. Total rate of glucose appearance (R_a Total) and disappearance (R_d) were determined from plasma [6,6-$^{2}H_2$]D-glucose enrichment. Rate of exogenous oral glucose appearance (R_a Oral) was determined from plasma [U-^{13}C]D-glucose enrichment [23]. Rate

of endogenous glucose appearance (R_a Endo) was calculated as the difference between R_a Total and R_a Oral.

Breath samples were also collected in 10mL vacutainers at -30 min, 0 min, and then every 30 min for 5h post-glucose ingestion to determine $^{13}CO_2$ enrichment, which permits estimation of glucose oxidation rate. These calculations require accurate measurement of oxygen consumption (inspired oxygen: VO_2), carbon dioxide production (expired carbon dioxide: VCO_2) and total volume of expired air all of which were acquired in a supine position using a gas analyzer system (TrueOne® 2400, ParvoMedics, East Sandy, UT, USA). Respiratory exchange ratio (RER) was calculated as VCO_2 / VO_2.

2.8 Beta cell function and insulin sensitivity

Indices of beta cell function and insulin sensitivity were assessed in all participants from the data acquired during the 300 min OGTT. A C-peptide minimal model method was used to estimate beta cell function (basal (Φ_b), static (Φ_s), dynamic (Φ_d) and global (Φ) pancreatic beta cell sensitivity to glucose), insulin sensitivity index (S_I) and the disposition index (DI: product of insulin secretion and insulin sensitivity) in response to an oral glucose load as described previously [24].

2.9 Statistical analyses

All data were normally distributed (Shapiro-Wilk test). Repeated measures ANOVA, including order as a between subjects factor, was used to examine treatment effects of RVX-208 on clinical characteristics, plasma metabolites, lipoprotein particle characteristics, lipid species, beta cell function/insulin sensitivity and glucose kinetics. Data are presented as mean ± SD in tables and mean ± SEM in figures. Analyses were conducted using SPSS (version

15; SPSS, Chicago, IL, USA) or MATLAB (version R2013a). Statistical significance was declared at $P \leq 0.05$. Benjamini-Hochberg (BH) methods were used to control for false discovery rate and correct for multiple corrections in all lipidomic analyses [25].

3. Results

3.1 Baseline characteristics

At screening, participants were either overweight or obese (BMI 30 ± 4kg/m^2) and had impaired glucose tolerance, with three individuals also presenting with impaired fasting glucose. Average glycated hemoglobin (HbA_{1c}) was 5.8 ± 0.4% (39.9 ± 4.5mmol/mol) and circulating HDL-C was 1.0 ± 0.2mmol/L. A summary of the baseline characteristics is presented in Table 1.

3.2 Clinical measures

Adherence to medication regimens based on pill counts was high (>98%) and not different between interventions (Table 2). There was no difference in plasma apoA-I, apolipoprotein A-II (apoA-II) or HDL-C concentrations between the treatment groups. There was also no effect of RVX-208 treatment on other conventional clinical plasma lipids measures including total cholesterol, LDL-cholesterol (LDL-C) or TG (Table 2).

3.3 Lipidomic analysis of the HDL fraction

Following normalization of the HDL lipid measures to apoA-I content, there was a significant increase in 12 of the 24 lipid classes in the HDL fraction after RVX-208 treatment, 10 of which remained significant after correction for multiple comparisons (Table 3). These predominantly surface lipids included ceramide (Cer), monohexosylceramide (MHC), dihexosylceramide (DHC), trihexosylceramide (THC), GM3 ganglioside (GM3), sphingomyelin (SM), alkylphosphatidylcholine (PC(O)), alkenylphosphatidylcholine (PC(P)), lysophosphatidylcholine (LPC) and lysophosphatidylethanolamine (LPE). Of the 342 lipid species detected in the HDL fraction, there was an increase in 77 individual lipid species (Supplemental Table 1). However, significance was lost after BH correction for multiple

comparisons. Similar to the lipid class analysis, these lipids consisted of mainly surface lipids (n=70), with only 7 core lipid species affected; 2 cholesteryl esters (CE), 2 diacylglycerols (DG) and 3 TG species. A large proportion of these individual lipids (n=44) were phosphatidylcholine (PC) species.

3.4 Lipoprotein particle size

RVX-208 treatment resulted in an 11% increase in the concentration of medium-sized HDL particles (P=0.01), a 10% decrease in small-sized HDL particles (P=0.04) and a 40% decrease in the concentration of total IDL particles (P=0.02) (Table 4). There was no treatment effect on the total HDL particle concentration, HDL particle size, LDL or VLDL/chylomicron particle concentration or total TG concentration (Table 4 and Supplemental Table 2).

3.5 Plasma glucose, insulin, C-peptide & incretin concentration

There was no change in fasting glucose (Placebo: 5.8 ± 0.6 vs RVX-208: 5.9 ± 0.6mmol/L) or fasting insulin (Placebo: 9.3 ± 6.2 vs RVX-208: 9.2 ± 5.2mU/L) between treatments. In response to a glucose load, plasma glucose concentration peaked at a similar concentration, but was delayed by 30 minutes after RVX-208 treatment with the elevation sustained for longer (P=0.003, Figure 2A). Similar to glucose, the peak insulin concentration was 30 minutes later following RVX-208 treatment vs placebo. However, there was no treatment effect on postprandial plasma insulin when analyzed during the entire OGTT (Figure 2B). The insulin:glucose concentration ratio was lower following RVX-208 compared to placebo treatment (P=0.021, Figure 2C). C-peptide concentrations closely mapped to the insulin time course with no overall treatment effect. There was an interaction between treatment and time (P=0.001), reflecting that later in the time course C-peptide concentrations were higher

following RVX-208 treatment when compared to placebo (Figure 2D). There was no treatment effect on fasting or post-glucose plasma incretin (GIP and GLP-1) concentrations (Supplemental Figure 2).

3.6 Glucose kinetics

Total glucose rate of appearance (R_a Total) was lower (P=0.001, Figure 3A) after RVX-208 vs placebo, as was the glucose rate of disappearance (R_d), an indirect measure of glucose uptake into tissues (P=0.016, Figure 3B). Endogenous glucose production (R_a Endo) was also marginally suppressed following RVX-208 treatment (P=0.014, Figure 3C). Also contributing to the lower glucose R_a Total was the reduction and delay in the appearance of the ingested glucose load (R_a Oral) in the circulation following RVX-208 treatment when compared to placebo (P=0.003, Figure 3D). Interestingly, there was no treatment effect on glucose oxidation during the OGTT (data not shown). However, glucose clearance (R_d/mean plasma glucose) was significantly lower after RVX-208 treatment vs placebo (Placebo: 2.52 ± 0.65mL/kg.min^{-1} vs RVX-208: 2.30 ± 0.49mL/kg.min^{-1}, P=0.019) when calculated over the entire OGTT.

3.7 Beta cell function and insulin sensitivity

Glucose, insulin and C-peptide concentrations across the entire time course were used as input data to determine indices of beta cell function and insulin sensitivity using a C-peptide oral minimal model. There was no effect of RVX-208 treatment on any of the parameters derived from this detailed modelling (Supplemental Table 3).

3.8 Safety assessments

RVX-208 treatment increased serum creatinine by 5% (P=0.006) with a trend for reduced estimated glomerular filtration rate (eGFR) (P=0.051, Supplemental Table 4). There was a small, but significant reduction in circulating chloride (P=0.04) and a corresponding trend for reduced plasma sodium (P=0.08). The red cell count was also 2% lower (P=0.04) after RVX-208 treatment, which may be related to a direct effect of the drug on renal function. Whilst these differences were statistically significant, it should be noted that all measures remained within normal clinical ranges. There were no significant drug effects on liver function test (LFT) measures when analyzed as a group (Supplemental Table 5).

4. Discussion

This is the first report showing that an orally active BET-inhibitor may modulate glucose metabolism using state-of-the-art isotope dilution methodologies. Four weeks of treatment with RVX-208 led to a reduction in the appearance of an oral glucose load in the circulation associated with reduced endogenous glucose production, balanced by reduced glucose disposal. The net effect in this population with prediabetes was a delayed, but also sustained peak in plasma glucose following a glucose challenge. The reduction in oral glucose absorption may be particularly clinically significant for individuals with already impaired glucose tolerance. RVX-208 also induced significant changes in HDL lipid composition and HDL particle size distribution, modifying HDL lipid classes towards a healthy lipid profile, and promoting a switch from small to medium-sized HDL particles. Interestingly, these changes occurred in the absence of any effect on conventional clinical lipid parameters, including plasma HDL-C and apoA-I. Our findings highlight both the limitations of clinical lipid parameters, but also reveal HDL modifications induced by short-term RVX-208 treatment, which may have functional implications. Whether the parallel effects on HDL particle size/composition and glucose metabolism are causally related however, cannot be directly determined in a clinical trial (Supplemental Figure 3).

4.1 RVX-208 and glucose metabolism

The peak in plasma glucose after the oral glucose load was of similar magnitude after RVX-208 and placebo, but was delayed and sustained following the active treatment. Plasma insulin and C-peptide responses mapped closely with this delay in peak plasma glucose. The resultant net reduction in the insulin:glucose ratio during the first 2 hours of the OGTT may suggest an increase in insulin sensitivity during this period. However, the oral minimal

modelling was unable to detect a treatment effect, most probably due to the fact that it was not sustained and that the modelling integrates data over the entire 5 hour OGTT period.

More detailed analyses of glucose kinetics were possible due to the dual stable isotope tracer methodologies employed. RVX-208 treatment resulted in a decrease in total, endogenous and oral glucose R_a, with a concomitant decrease in glucose R_d and no change in glucose oxidation rate. The reduced oral glucose R_a resulted in a delay in the peak plasma glucose and insulin by approximately 30 minutes. This reduction in appearance of the exogenous oral glucose load in the plasma may be due to: 1) reduced glucose absorption from the intestine into the circulation with or without reduced gastric emptying, 2) higher glucose utilization in the gastrointestinal tract and/or 3) higher hepatic glucose utilization or storage in the form of glycogen. The reduced uptake of the oral glucose load was accompanied by a small reduction in endogenous glucose production and both effects could arise due to primary effects of the drug on the intestine and/or liver. The reduced glucose R_d may also be compensatory to maintain blood glucose homeostasis.

One possible mechanism explaining a reduction in intestinal glucose absorption could be altered activity of the sodium glucose co-transporter, SGLT1 in intestinal enterocytes. Whilst speculative, this would be consistent with the observed trend for reduced plasma sodium after RVX-208 treatment, given that sodium ions and glucose would move in the same direction. SGLT1 is the predominant intestinal glucose transporter, functioning as a glucose sensor in enteroendocrine cells contributing to glucose-induced secretion of the incretins, GIP and GLP-1 [26]. Despite this, there was no effect of RVX-208 treatment on circulating incretin hormone concentrations either after fasting or post-glucose load.

4.2 RVX-208 and HDL

While HDL is known to modulate glucose metabolism [2], we cannot determine whether the effects of RVX-208 on glucose metabolism directly relate to the observed changes in the HDL lipidome. It is however interesting to note the effects of the intervention on HDL particle size and composition in the absence of any change in conventional lipid parameters.

We found that RVX-208 treatment induced a shift toward a larger HDL particle size as evidenced by an 11% increase in the concentration of medium-sized HDL particles and a 10% reduction in small HDL particles. These findings are in line with a previous study in a population with stable coronary artery disease (ASSERT trial) using the same dose of RVX-208 as in the current study, which showed a 21.1% increase in the concentration of large HDL particles following 12 weeks of treatment [14]. HDL particle size is mainly influenced by core lipids, including CE, DG and TG. The shift from smaller to larger particles may signal a modification of HDL metabolism, possibly by a reduction in CETP activity and/or an increase in cholesterol efflux from peripheral cells. Growth in particle size can also be driven by lecithin-cholesterol acyltransferase (LCAT), which converts unesterified cholesterol effluxed from peripheral cells into CE stored within the core of HDL particles. We found that the RVX-208-induced changes in HDL particle size were not associated with significant increases in the concentration of core lipid species in the collective HDL lipidome, though trends were evident. The absence of changes in core lipids including CE, TG and the ratio of CE to unesterified cholesterol however argue against changes in CETP or LCAT activity. This has been supported by a previous phase I trial conducted by Resverlogix showing no effect of RVX-208 treatment for 28 days on plasma CETP or LCAT concentrations at a dose of 1mg/kg b.i.d which corresponds to the therapeutic dose used in our current study (100mg b.i.d) (unpublished data). Despite this, the idea that RVX-208 might promote reverse

cholesterol transport is certainly supported by *in vitro* cholesterol efflux assays [11] and previous studies involving apoA-I infusion [27]. It is also consistent with the recent report that 150mg/kg b.i.d RVX-208 for 12 weeks reduces aortic lesion formation in apolipoprotein E (apoE) knockout mice along with a 2-fold increase in circulating HDL-C, suggesting a combination of cholesterol efflux and anti-inflammatory actions [28].

Beyond the effects of RVX-208 on HDL particle concentration and size, 10 lipid classes were increased within the HDL lipidome. Included in these were 6 sphingolipid (Cer, MHC, DHC, THC, GM3, SM) and 4 phospholipid (PC(O), PC(P), LPC, LPE) classes. These HDL composition changes can be put in context of our recent finding that HDL isolated from individuals with metabolic syndrome had lower total Cer, MHC, THC, SM, PC(P) and PC(O) when compared to healthy controls [29]. Modification of the HDL lipidome towards the profile observed in healthy controls may also modulate the multiple anti-atherothrombotic functions of HDL through a number of well-established mechanisms [30-32].

Ceramides were prominent amongst the sphingolipids modulated by RVX-208 treatment and play a diverse role in the pathogenesis of T2DM and cardiovascular disease, but are also precursors of more complex sphingolipids, which mediate cardiometabolic protection. We have previously shown that insulin-sensitive obese individuals have higher levels of total Cer in the isolated HDL fraction than those obese individuals who develop T2DM [33]. These data raise the possibility that elevation of HDL-bound Cer may protect against insulin resistance. Such effects could potentially be conveyed via HDL-mediated transport of Cer to the liver for excretion. Alternatively, Cer is a precursor of sphingosine-1-phosphate (S1P) which functions as a ligand for G protein-coupled S1P receptors in numerous cell types, regulating multiple cell functions including glucose metabolism [31].

4.3 Strengths

This is the first report showing that an orally active BET-inhibitor modulates glucose metabolism using a robust randomized, placebo controlled study design with state-of-the-art methodologies to assess glucose metabolism and the HDL lipidome. Detailed analyses of glucose kinetics, including oral absorption, were possible due to the dual stable isotope tracer methodologies employed. Our findings highlight both the limitations of conventional clinical lipid parameters, but also show the strengths of lipidomic analyses to characterize HDL compositional changes induced by short-term RVX-208 treatment.

4.4 Weaknesses/Limitations

In a clinical trial of this nature, we cannot determine whether the observed effects of RVX-208 on HDL particle size and composition are causative in relation to the observed effects on glucose metabolism. A mechanistic animal study would be required to further elucidate any direct causative relationship.

4.5 Translational potential

The delay and reduction in oral glucose absorption and endogenous glucose production induced by RVX-208 are potentially clinically significant in protecting against progression to type 2 diabetes, though longer term studies are required. Our study highlights the importance of examining the effects of lipid-modifying agents on the lipidome of individual lipoprotein classes to permit elucidation of composition-function relationships important for informing future therapeutic development. For example, modification of the HDL lipidome towards the profile observed in healthy controls may favour multiple beneficial actions of HDL.

4.6 Conclusions

This is the first evidence that 4 weeks of RVX-208 treatment is sufficient to induce subtle changes in glucose metabolism, in association with changes in the HDL lipidome. RVX-208 delayed and reduced the appearance of oral glucose in the circulation in association with reduced endogenous glucose production. This was accompanied by a reduction in glucose disposal, which acted to sustain peak plasma glucose following RVX-208 treatment. RVX-208 also altered the HDL lipidome, increasing lipid classes that are generally lower in metabolic disease states, and promoting a switch from small to medium-sized HDL particles.

Acknowledgements

The authors would like to thank Dr. Wayne Childs, Donna Vizi and Jenny Starr (Alfred Hospital, Cardiology Department, Melbourne, Victoria, Australia) for their technical assistance and the research participants for their time and interest in our study. This was an investigator-initiated project. Whilst Resverlogix Corp. was permitted to review the manuscript and suggest changes, they played no role in data analysis.

Funding

This study was supported by Resverlogix Corp., the National Health & Medical Research Council (NHMRC) of Australia (APP1065462) to BAK, SJD and ALS, and in part by the Victorian Government's Operational Infrastructure Support (OIS) Program. BAK, DS and PJM are all supported by NHMRC Research Fellowships.

Disclosure statement

JJ & NCWW are employees, share- and option holders of Resverlogix Corporation. JDO is employed by LabCorp. BAK received a research grant and travel support from Resverlogix Corporation.

Author contributions

ALS, MFF, GVH, KAR, JJ, AG, NCWW, DS, PB, SJD, PJM and BAK were involved in the conception and design of the study. ALS, SKT, MFF, AKN, MR, ALC and SJD were involved in acquisition of data. ALS, SKT, PAM, KH, AAK, ALC, GVH, CC, CD, JDO, KAR, PJM and BAK were involved in analysis and interpretation of data. ALS, SKT and BAK drafted the article. All authors revised the article critically for important intellectual content and gave final approval of the version to be submitted.

References

[1] Drew BG, Duffy SJ, Formosa MF, Natoli AK, Henstridge DC, Penfold SA, et al. High-density lipoprotein modulates glucose metabolism in patients with type 2 diabetes mellitus. Circulation. 2009;119:2103-11.

[2] Drew BG, Rye KA, Duffy SJ, Barter P, Kingwell BA. The emerging role of HDL in glucose metabolism. Nat Rev Endocrinol. 2012;8:237-45.

[3] Barter PJ, Rye KA, Tardif JC, Waters DD, Boekholdt SM, Breazna A, et al. Effect of Torcetrapib on Glucose, Insulin, and Hemoglobin A1c in Subjects in the Investigation of Lipid Level Management to Understand its Impact in Atherosclerotic Events (ILLUMINATE) Trial. Circulation. 2011;124:555-62.

[4] Fryirs MA, Barter PJ, Appavoo M, Tuch BE, Tabet F, Heather AK, et al. Effects of high-density lipoproteins on pancreatic beta-cell insulin secretion. Arterioscler Thromb Vasc Biol. 2010;30:1642-8.

[5] Siebel AL, Natoli AK, Yap FY, Carey AL, Reddy-Luthmoodoo M, Sviridov D, et al. Effects of high-density lipoprotein elevation with cholesteryl ester transfer protein inhibition on insulin secretion. Circ Res. 2013;113:167-75.

[6] Carey AL, Siebel AL, Reddy-Luthmoodoo M, Natoli AK, D'Souza W, Meikle PJ, et al. Skeletal muscle insulin resistance associated with cholesterol-induced activation of macrophages is prevented by high density lipoprotein. PLoS One. 2013;8:e56601.

[7] Rohatgi A, Khera A, Berry JD, Givens EG, Ayers CR, Wedin KE, et al. HDL cholesterol efflux capacity and incident cardiovascular events. N Engl J Med. 2014;371:2383-93.

[8] Kingwell BA, Chapman MJ, Kontush A, Miller NE. HDL-targeted therapies: progress, failures and future. Nat Rev Drug Discov. 2014;13:445-64.

[9] Camont L, Lhomme M, Rached F, Le Goff W, Negre-Salvayre A, Salvayre R, et al. Small, dense high-density lipoprotein-3 particles are enriched in negatively charged

phospholipids: relevance to cellular cholesterol efflux, antioxidative, antithrombotic, anti-inflammatory, and antiapoptotic functionalities. Arterioscler Thromb Vasc Biol. 2013;33:2715-23.

[10] Kingwell BA, Chapman MJ. Future of high-density lipoprotein infusion therapies: potential for clinical management of vascular disease. Circulation. 2013;128:1112-21.

[11] Bailey D, Jahagirdar R, Gordon A, Hafiane A, Campbell S, Chatur S, et al. RVX-208: a small molecule that increases apolipoprotein A-I and high-density lipoprotein cholesterol in vitro and in vivo. J Am Coll Cardiol. 2010;55:2580-9.

[12] McLure KG, Gesner EM, Tsujikawa L, Kharenko OA, Attwell S, Campeau E, et al. RVX-208, an inducer of ApoA-I in humans, is a BET bromodomain antagonist. PLoS One. 2013;8:e83190.

[13] Picaud S, Wells C, Felletar I, Brotherton D, Martin S, Savitsky P, et al. RVX-208, an inhibitor of BET transcriptional regulators with selectivity for the second bromodomain. Proc Natl Acad Sci U S A. 2013;110:19754-9.

[14] Nicholls SJ, Gordon A, Johansson J, Wolski K, Ballantyne CM, Kastelein JJ, et al. Efficacy and safety of a novel oral inducer of apolipoprotein a-I synthesis in statin-treated patients with stable coronary artery disease a randomized controlled trial. J Am Coll Cardiol. 2011;57:1111-9.

[15] Breda E, Cavaghan MK, Toffolo G, Polonsky KS, Cobelli C. Oral glucose tolerance test minimal model indexes of beta-cell function and insulin sensitivity. Diabetes. 2001;50:150-8.

[16] Patel S, Drew BG, Nakhla S, Duffy SJ, Murphy AJ, Barter PJ, et al. Reconstituted high-density lipoprotein increases plasma high-density lipoprotein anti-inflammatory properties and cholesterol efflux capacity in patients with type 2 diabetes. J Am Coll Cardiol. 2009;53:962-71.

[17] Eugui J, Logrono MJ, Ruiz R, Zugaza C, Mirabel JL, Martinez C. Immunoturbidimetry of serum apolipoproteins A-I and B on the Cobas Bio centrifugal analyzer: method validation and reference values. Clinical biochemistry. 1994;27:310-5.

[18] Havel RJ, Eder HA, Bragdon JH. The distribution and chemical composition of ultracentrifugally separated lipoproteins in human serum. J Clin Invest. 1955;34:1345-53.

[19] Otvos JD, Mora S, Shalaurova I, Greenland P, Mackey RH, Goff DC, Jr. Clinical implications of discordance between low-density lipoprotein cholesterol and particle number. J Clin Lipidol. 2011;5:105-13.

[20] Oehlke J, Brudel M, Blasig IE. Benzoylation of sugars, polyols and amino acids in biological fluids for high-performance liquid chromatographic analysis. Journal of chromatography B, Biomedical applications. 1994;655:105-11.

[21] Knudsen SH, Karstoft K, Pedersen BK, van Hall G, Solomon TP. The immediate effects of a single bout of aerobic exercise on oral glucose tolerance across the glucose tolerance continuum. Physiological reports. 2014;2.

[22] Steele R. Influences of glucose loading and of injected insulin on hepatic glucose output. Ann N Y Acad Sci. 1959;82:420-30.

[23] Proietto J. Estimation of glucose kinetics following an oral glucose load. Methods and applications. Hormone and metabolic research Supplement series. 1990;24:25-30.

[24] Cobelli C, Dalla Man C, Toffolo G, Basu R, Vella A, Rizza R. The oral minimal model method. Diabetes. 2014;63:1203-13.

[25] Hochberg Y, Benjamini Y. More powerful procedures for multiple significance testing. Statistics in medicine. 1990;9:811-8.

[26] Roder PV, Geillinger KE, Zietek TS, Thorens B, Koepsell H, Daniel H. The role of SGLT1 and GLUT2 in intestinal glucose transport and sensing. PLoS One. 2014;9:e89977.

[27] Kujiraoka T, Nanjee MN, Oka T, Ito M, Nagano M, Cooke CJ, et al. Effects of intravenous apolipoprotein A-I/phosphatidylcholine discs on LCAT, PLTP, and CETP in plasma and peripheral lymph in humans. Arterioscler Thromb Vasc Biol. 2003;23:1653-9.

[28] Jahagirdar R, Zhang H, Azhar S, Tobin J, Attwell S, Yu R, et al. A novel BET bromodomain inhibitor, RVX-208, shows reduction of atherosclerosis in hyperlipidemic ApoE deficient mice. Atherosclerosis. 2014;236:91-100.

[29] Khan AA, Straznicky NE, Nestel PJ, Wong G, Mundra PA, Mellett NA, et al. Effect of weight loss and exercise on the high-density lipoprotein (HDL) lipidome in individuals with metabolic syndrome (MetS). 83rd European Atherosclerosis Society (EAS) Congress. Glasgow, UK2015.

[30] Annema W, von Eckardstein A. High-density lipoproteins. Multifunctional but vulnerable protections from atherosclerosis. Circulation journal : official journal of the Japanese Circulation Society. 2013;77:2432-48.

[31] Poti F, Simoni M, Nofer JR. Atheroprotective role of high-density lipoprotein (HDL)-associated sphingosine-1-phosphate (S1P). Cardiovasc Res. 2014;103:395-404.

[32] Lucero D, Svidirov D, Freeman L, Lopez GI, Fassio E, Remaley AT, et al. Increased cholesterol efflux capacity in metabolic syndrome: Relation with qualitative alterations in HDL and LCAT. Atherosclerosis. 2015;242:236-42.

[33] Boon J, Hoy AJ, Stark R, Brown RD, Meex RC, Henstridge DC, et al. Ceramides contained in LDL are elevated in type 2 diabetes and promote inflammation and skeletal muscle insulin resistance. Diabetes. 2013;62:401-10.

Table 1. Baseline characteristics

Characteristic	
Age (years)	**57 ± 7**
Height (cm)	**177.0 ± 7.2**
Weight (kg)	**94.3 ± 14.6**
BMI (kg/m^2)	**30 ± 4**
Systolic blood pressure (mmHg)	**123 ± 12**
Diastolic blood pressure (mmHg)	**79 ± 7**
Total cholesterol (mmol/L)	**5.3 ± 1.0**
HDL-C (mmol/L)	**1.0 ± 0.2**
LDL-C (mmol/L); #n=19	**3.4 ± 0.8**
TG (mmol/L)	**1.9 ± 1.5**
HbA1c (%)	**5.8 ± 0.4**
HbA1c (mmol/mol)	**39.9 ± 4.5**
Fasting insulin (mU/L)	**9.3 ± 4.5**
Fasting glucose (mmol/L)	**5.6 ± 0.4**
120min OGTT glucose (mmol/L)	**9.2 ± 1.0**

Data presented as mean ± SD, n=20 unless otherwise stated. #Calculation of LDL-C invalid in n=1 individual, where TG > 4.5 mmol/L.

Table 2. Clinical measures

Parameter	Pre-Placebo	Post-Placebo	Change	Pre-RVX-208	Post-RVX-208	Change	*P*-value treatment (trt)	*P*-value order	*P*-value trt x order
Treatment duration (days)		34.7 ± 1.6			34.8 ± 1.2		0.87	0.11	0.43
Adherence (%)		98.5 ± 2.3			98.1 ± 3.2		0.21	0.72	0.32
Total cholesterol (mmol/L)	5.34 ± 0.98	5.31 ± 0.80	**-0.04 ± 0.40**	5.51 ± 1.12	5.17 ± 0.82	**-0.35 ± 0.83**	0.13	0.63	0.32
HDL-C (mmol/L)	1.09 ± 0.23	1.07 ± 0.18	**-0.03 ± 0.10**	1.13 ± 0.21	1.09 ± 0.20	**-0.04 ± 0.13**	0.79	0.48	0.05
LDL-C (mmol/L); #n=18	3.40 ± 0.93	3.40 ± 0.67	**0.001 ± 0.44**	3.46 ± 0.90	3.34 ± 0.73	**-0.11 ± 0.55**	0.40	0.91	0.14
TG (mmol/L)	1.76 ± 1.05	1.75 ± 1.00	**-0.01 ± 0.50**	1.74 ± 0.98	1.70 ± 1.02	**-0.04 ± 0.90**	0.91	0.26	0.30
ApoA-I (mg/dL)	129.7 ± 14.7	127.7 ± 11.3	**-2.05 ± 6.40**	130.8 ± 11.7	127.6 ± 13.8	**-3.25 ± 9.68**	0.68	0.50	0.95
ApoA-II (mg/dL)	40.9 ± 4.19	41.1 ± 3.50	**0.24 ± 3.00**	41.7 ± 4.30	41.3 ± 4.47	**-0.38 ± 2.78**	0.56	0.87	0.08
hsCRP (mg/L)	2.58 ± 1.93	1.93 ± 1.49	**-0.66 ± 1.80**	2.02 ± 1.78	1.98 ± 1.63	**-0.04 ± 0.82**	0.26	0.99	0.83
Fructosamine (µmol/L)	223 ± 18	218 ± 25	**-5 ± 18**	223 ± 21	222 ± 18	**-2 ± 20**	0.58	0.12	0.17

Data are presented as mean ± SD, n=20 unless otherwise stated, *P*-values from Repeated Measures ANOVA. #Calculation of LDL-C invalid in n=2 individuals, where TG > 4.5 mmol/L.

Table 3. HDL fraction lipid classes

Lipids	Placebo	RVX-208	Mean % change	*P*-value treatment (trt)	BH corrected *P*-value trt	*P*-value order	*P*-value trt x order
dhCer	0.11 ± 0.05	0.12 ± 0.03	**29.8 ± 49.0**	0.08	0.15	0.52	0.62
Cer	0.29 ± 0.06	0.34 ± 0.07	**20.9 ± 29.0**	0.01*	0.05#	0.24	0.12
MHC	2.01 ± 0.35	2.33 ± 0.43	**17.6 ± 22.9**	0.01*	0.04#	0.59	0.96
DHC	1.46 ± 0.38	1.66 ± 0.44	**15.7 ± 23.7**	0.02*	0.05#	0.99	0.48
THC	0.46 ± 0.10	0.55 ± 0.15	**21.2 ± 30.0**	0.01*	0.04#	0.47	0.33
GM3	0.87 ± 0.18	1.06 ± 0.19	**23.4 ± 23.3**	0.001*	0.01#	0.44	0.40
SM	60.5 ± 10.7	68.3 ± 12.1	**14.5 ± 21.6**	0.02*	0.05#	0.56	0.18
PC	595 ± 135	696 ± 201	**19.8 ± 33.9**	0.04*	0.10	0.87	0.24
PC(O)	19.6 ± 4.29	22.8 ± 4.72	**18.6 ± 25.4**	0.01*	0.04#	0.42	0.84
PC(P)	10.1 ± 2.30	11.8 ± 2.39	**18.4 ± 23.9**	0.01*	0.04#	0.29	0.99
LPC	8.79 ± 2.83	10.2 ± 3.69	**16.3 ± 22.2**	0.02*	0.05#	0.50	0.40
LPC(O)	0.42 ± 0.07	0.48 ± 0.09	**15.1 ± 27.0**	0.05*	0.10	0.44	0.65
PE	7.89 ± 1.87	9.23 ± 3.08	**20.9 ± 42.8**	0.11	0.18	0.02*	0.56
PE(O)	0.94 ± 0.25	1.03 ± 0.39	**13.5 ± 41.2**	0.31	0.37	0.70	0.37
PE(P)	1.27 ± 0.25	1.45 ± 0.47	**16.1 ± 38.2**	0.14	0.21	0.89	0.42
LPE	0.74 ± 0.20	0.90 ± 0.32	**23.4 ± 33.9**	0.01*	0.05#	0.07	0.36
PI	12.5 ± 2.39	13.5 ± 3.91	**9.8 ± 32.2**	0.31	0.37	0.21	0.61
LPI	0.04 ± 0.02	0.05 ± 0.02	**18.3 ± 43.2**	0.54	0.59	0.68	0.55
PS	0.58 ± 0.47	0.58 ± 0.50	**75.9 ± 192**	0.96	0.96	0.47	0.46
PG	0.11 ± 0.05	0.11 ± 0.05	**16.9 ± 56.0**	0.86	0.90	0.38	0.49

COH	103 ± 19.8	112 ± 27.2	**12.4 ± 40.4**	0.28	0.37	0.45	0.40
CE	2640 ± 531	2900 ± 469	**12.9 ± 26.2**	0.12	0.19	0.89	0.95
DG	3.52 ± 0.86	3.88 ± 1.15	**12.8 ± 31.0**	0.15	0.22	0.36	0.26
TG	17.8 ± 4.59	19.0 ± 6.21	**8.9 ± 29.3**	0.37	0.42	0.28	0.42

Data are presented as mean ± SD and normalized to apoA-I (nmol/mg apoA-I), n=18, *P*-values from Repeated Measures ANOVA. *$P \leq 0.05$; #$P \leq 0.05$ after Benjamini-Hochberg (BH) correction.

Table 4. NMR spectroscopy lipoprotein parameters

Parameter	Pre-Placebo	Post-Placebo	Change	Pre-RVX-208	Post-RVX-208	Change	*P*-value treatment (trt)	*P*-value order	*P*-value trt x order
Total IDL particles (nmol/L)	155 ± 108	166 ± 102	**11 ± 109**	218 ± 136	131 ± 90	**-87 ± 129**	0.02*	0.45	0.12
Total HDL particles (µmol/L)	31.2 ± 4.0	30.1 ± 3.0	**-1.1 ± 2.9**	31.3 ± 3.6	30.7 ± 4.1	**-0.6 ± 3.5**	0.67	0.03*	0.39
Large HDL particles (µmol/L)	3.0 ± 1.4	3.2 ± 1.2	**0.2 ± 1.1**	2.9 ± 1.2	3.2 ± 1.5	**0.3 ± 0.9**	0.79	0.06	0.11
Medium HDL particles (µmol/L)	8.3 ± 3.8	6.7 ± 3.3	**-1.6 ± 2.3**	8.4 ± 4.0	9.5 ± 4.4	**1.1 ± 2.8**	0.01*	0.30	0.19
Small HDL particles (µmol/L)	20.0 ± 4.7	20.3 ± 3.9	**0.3 ± 2.7**	20.0 ± 3.3	18.0 ± 4.1	**-2.0 ± 3.4**	0.04*	0.59	0.81
Total HDL-C (mg/dL)	41.0 ± 6.3	39.4 ± 4.7	**-1.6 ± 3.6**	40.4 ± 5.3	40.8 ± 5.9	**0.4 ± 3.8**	0.14	0.02*	0.88
HDL size (nm)	8.7 ± 0.2	8.7 ± 0.3	**0.001 ± 0.3**	8.6 ± 0.2	8.7 ± 0.3	**0.1 ± 0.2**	0.12	0.03*	0.10
Total TG (mg/dL)	158 ± 90	154 ± 82	**-4.7 ± 36.4**	158 ± 91	149 ± 81	**-9.8 ± 79.0**	0.82	0.34	0.24

Data are presented as mean ± SD, n=20, *P*-values from Repeated Measures ANOVA. *$P < 0.05$.

Figure legends

Figure 1. Study design diagram. fsOGTT: frequently sampled oral glucose tolerance test.

Figure 2. Glucose, insulin and C-peptide concentration. Circulating plasma A) glucose (mmol/L), B) insulin (mU/L), C) glucose:insulin and D) C-peptide (pmol/L) concentration measured from time 0 min through to the end of the OGTT (75g glucose bolus) procedure (300 minutes) at visit 3 and visit 6, corresponding to either placebo (open circles) or RVX-208 (closed squares). Data are presented as mean ± SEM, n=20. Repeated measures ANOVA was used to test for significant differences across the timecourse between groups; main effect of treatment **P* < 0.05, ***P* < 0.01; #*P* < 0.01 interaction effect (treatment x time).

Figure 3. Glucose kinetics. A) Total glucose rate of appearance (R_a Total, μmol/kg.min^{-1}), B) total glucose rate of disappearance (R_d, μmol/kg.min^{-1}), C) endogenous glucose production (R_a Endo, μmol/kg.min^{-1}) and D) oral glucose rate of appearance (R_a Oral, μmol/kg.min^{-1}) were calculated following intravenous infusion of [6,6-$^{2}H_2$]D-glucose 120 min before a glucose load containing [U-$^{13}C_6$]D-glucose ingested at time 0 min through to the end of the OGTT (75g glucose bolus) procedure (300 minutes) at visit 3 and visit 6, corresponding to either placebo (open circles) or RVX-208 (closed squares). Data are presented as mean ± SEM, n=20. Repeated measures ANOVA was used to test for significant differences across the timecourse between groups; main effect of treatment **P* < 0.05, ***P* < 0.01.

Figure 1

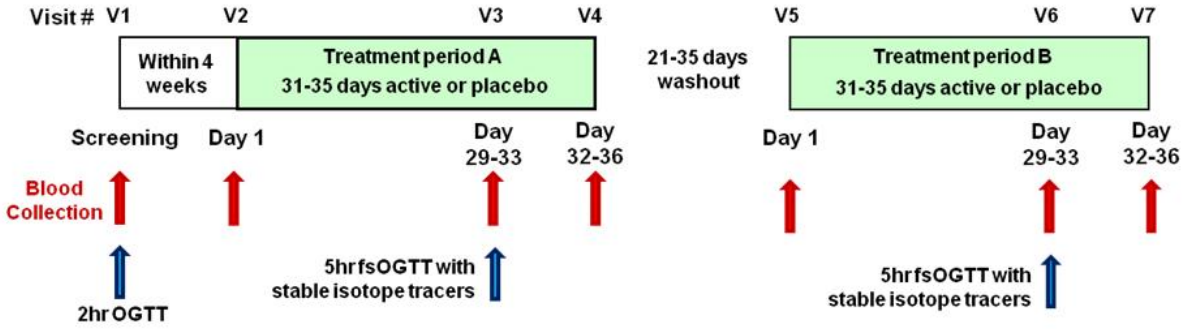

Figure 2

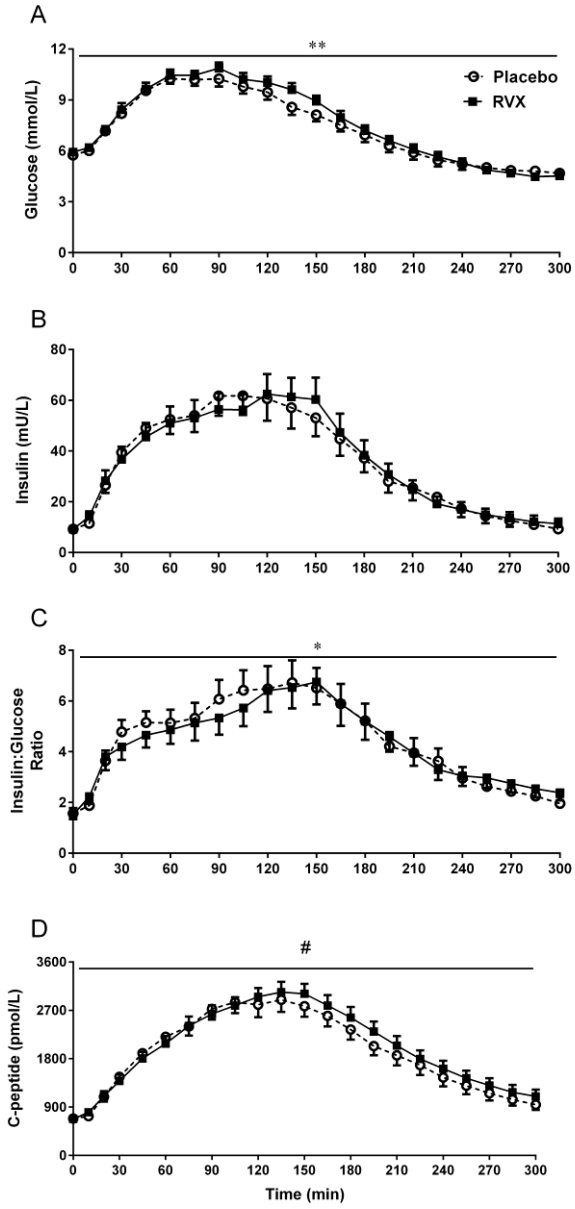

Figure 3